Charged Particle Induced Noise in Camera Systems

Carl Christian Liebe

Jet Propulsion Laboratory, California Institute of Technology

4800 Oak Grove Dr, Pasadena Ca. 91101

Abstract: When a camera system is operated in a flux of charged particles, it will generate a transient signal. The charged particles will impinge on the focal plane array and generate tracks of ionized electron-hole pairs. The charge tracks will diffuse and some of the charge will be collected as signal and the rest will recombine. Bremsstrahlung will be generated in the structure around the camera and the Bremsstrahlung photons will interact with the focal plane array. The charged particles will also make the optics "glow" due to Luminescence and Cerenkov radiation. This paper utilizes a charged particle flux found in open literature, for a future spacecraft called Europa Orbiter to show the effects of charged particles on a camera system. A simple focal plane model is constructed based on typical values and the simulations of the transient noise will be discussed. The radiation will look like small stars. In this specific simulation the radiation will generate average values of 3600 photoelectrons for impinging electrons, 6000 photoelectrons for impinging Bremsstrahlung photons and 15000 photoelectrons for impinging protons.

I. INTRODUCTION

In some space applications, it is desired to have visual imagery in environments with a high flux of charged particles, e.g. in the Van Allen belts or in the vicinity of Jupiter. The charged particles will influence the electronics of the camera system in three ways:

- **Ionizing damage**: Ionization damage is a cumulative damage. It occurs when the absorbed radiation energy goes into forming electron-hole pairs. Ionizing dose is normally measured as the energy absorbed per unit mass of material, with 1 rad defined as 100 erg/g [1]. The dose per unit of fluence depends on the type and energy of the radiation, and on the material being irradiated. Therefore, values of ionizing dose must be referenced to a particular material, e.g. Rad(Si). In silicon, one electron-hole pair is formed for every 3.6 eV absorbed [2]. In a camera system, the ionizing damage causes increased surface generated dark current and flat band voltage shifts in the focal plane array [3].

- **Displacement damage**: Displacement damage is a cumulative damage. It occurs when silicon atoms are displaced from the silicon lattice. This causes vacancies and interstitial silicon atoms, which can produce energy states within the bandgap. The production of displacements is an inherent property of radiation and a silicon lattice, making it relatively technology independent. Displacement damage is also referred to as Non Ionizing Energy Loss (NIEL) [4]. In a focal plane array, displacement damage typically cause increased dark current, hot pixels and in the case of CCD's reduced Charge Transfer Efficiency [3].

- **Transient effects:** Transient effects come from the momentary presence of electron-hole pairs produced by ionizing radiation. Collection of one or the other of these carrier types places an (approximately) instantaneous charge on some node of a circuit, impacting the operation of the circuit. In the case of a silicon focal plane array, this will generate bright spots on the pixels and increased noise [3].

This work will focus on the transient signals generated in a camera system by charged particles. For discussions on ionizing dose and displacement damage, refer to e.g. [3]. The charged particle flux may cause increased transient noise in the analog signal chain of the camera system and cause latch-up in the digital control electronics. However, the primary transient radiation impact will be on the focal plane itself and in the optics.

A charged particle flux was found in the open literature for a future spacecraft called Europa Orbiter [5]. This is used as an example in this paper, but the theory and the model are also applicable to any other charged particle environment. The electron and proton fluxes behind 5 g/cm^2 of aluminum are shown in figure 1 and figure 2. The total dose for the Bremsstrahlung is estimated to be 20Krad(Si) behind 5 g/cm^2 of aluminum shielding [5].

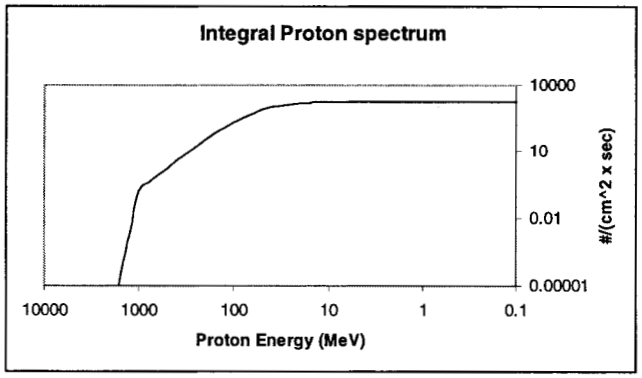

Figure 1. The estimated integral proton flux for the Europa Orbiter mission.

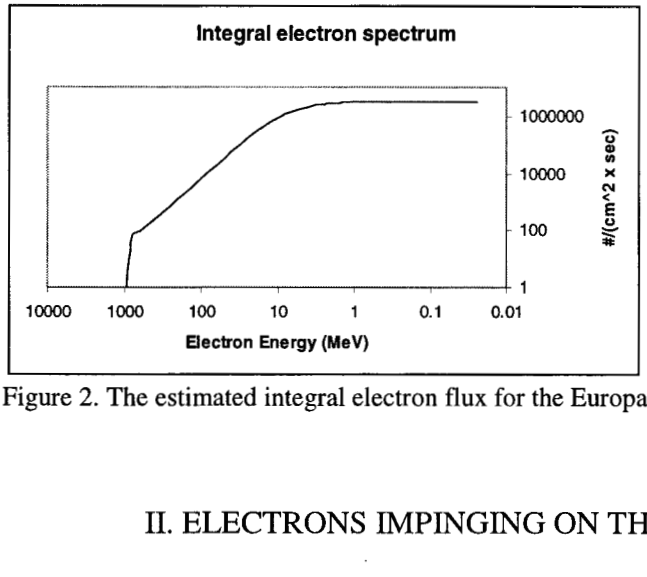

Figure 2. The estimated integral electron flux for the Europa Orbiter mission.

II. ELECTRONS IMPINGING ON THE FOCAL PLANE ARRAY

An electron traveling in a silicon lattice interacts primarily though Coulomb forces with the positive silicon nuclides and the negative orbiting electrons. Due to these many interactions, an electron loses energy and changes its trajectory continuous. The energy loss per distance is often referred to as Linear Energy Transfer (LET). The formulas for LET can be found in [6]. It is shown graphically in figure 3.

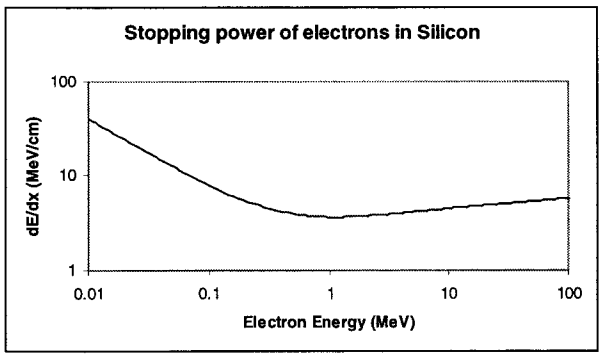

Figure 3. LET of electrons in silicon.

When electrons are traveling though silicon, they are continually deflected in the trajectory due to the attraction and repulsion from the electric field generated by the nuclei and by the electrons in the silicon lattice. Considerable effort has gone into the formulation of a theory of Coulomb multiple scattering. The program NOVICE[1] has provided the average scattering angles shown in figure 4.

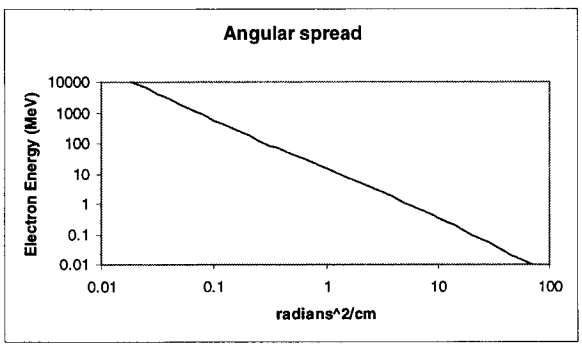

Figure 4. Average scattering angle for electrons in silicon.

Multiple Coulomb scattering is a cumulative statistical superposition of a huge number of small deflections [6]. Therefore the distribution of deflection angles follows a normal distribution. On rare occasions, the electrons may also collide with an atomic electron/nuclei and loose all their energy in one collision. Electrons may therefore also be scattered to a larger angle [7]. This is called single scattering.

---

[1] http://see.msfc.nasa.gov/see/ire/model_novice.html#description

Based on the LET function and the deflection distribution, it is possible to make a Monte Carlo simulation of an electron traveling in silicon. This is done by selecting arbitrary electrons from the electron flux in figure 2. A random orientation, from which the electron will impinge on the silicon lattice, is also chosen. The electron travels in a straight line for a small incremental step. Then the deposited energy is calculated for the step and subtracted from the original energy. Now the direction of the trajectory is changed according to the angular deflection distribution. The electron travels a small step again and the procedure repeats itself until the electron has lost all energy. This is shown below.

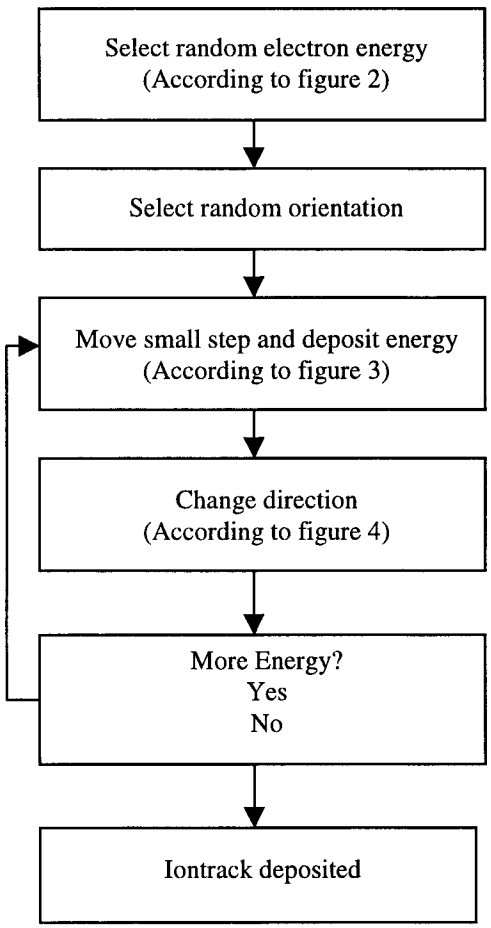

The trajectory of an electron, when it travels in silicon is called an ion track. The energy that the electron looses while traversing in silicon is deposited near the ion track in a complicated process [8]. The result of the process is that one electron hole pair is generated near the iontrack for each 3.6 eV deposited.

Carriers generated by ionizing radiation near the charge track will tend to spread out, as a result of their random thermal motion. This is called charge diffusion [8]-[13]. The diffusion length depends on the temperature, the carrier mobility and the carrier lifetime. Typically the lifetime of a carrier is less than 1 mS. The exposure time for a low light camera system will be orders of magnitude more. It can therefore be assumed (with good approximation) that when a carrier is generated, the camera will continue to expose for the rest of the carrier's life. It is therefore possible to simulate the charge diffusion for each carrier individually and independent of time [14]. This is achieved by having each minority carrier perform a random walk in 3 dimensions. The algorithm is shown below:

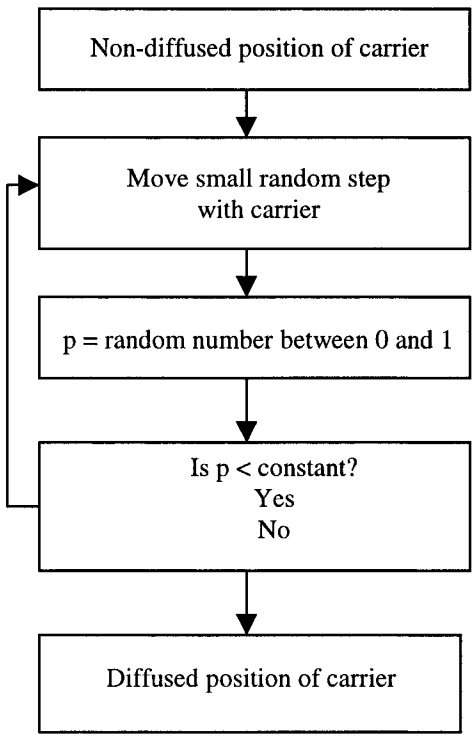

The value of the constant will determine the average diffusion length of the carrier before recombining. It depends on the step size and should be chosen to match the average diffusion length.

III. PROTONS IMPINGING ON THE FOCAL PLANE ARRAY

The mechanisms when protons travels in a silicon lattice are similar to when electrons travels in a silicon lattice. The major difference is that protons are heavier than electrons. The equations for energy loss due to ionization (LET) are shown in [6]. It is shown graphically in figure 5.

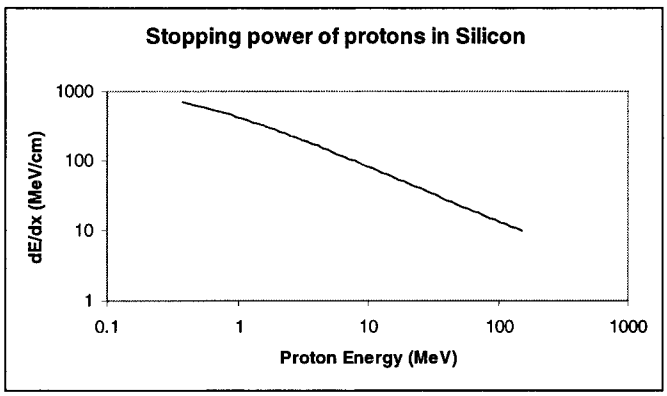

Figure 5. LET of protons in silicon.

When protons are traveling in silicon, they are continually deflected in their trajectory due to the attraction and repulsion from the electric field generated by the nuclei and by the electrons in the silicon lattice. However, the mass of the proton is so large that the deflections are very small. Therefore the proton trajectory deflections are neglected in this work. The energy that the proton looses while traveling in the silicon lattice is deposited near the ion track in a manner equivalent to that of electrons. The electron hole pairs also diffuse similar to the description in the previous section.

IV. BREMSSTRAHLUNG GENERATION

The focal plane array is surrounded by a structure. If the camera is designed to operate in a radiation environment, there will probably also be some additional shielding around the focal plane array. This will be designed to minimize the total accumulated dose and the transient signal generated by the charged particle flux.

When charged particles are impinging on the structure/shielding (e.g. aluminum, wolfram or glass), the charged particles will be decelerated. When a charged particle is decelerated, it emits photons. This radiation is called Bremsstrahlung. The intensity of Bremsstrahlung is proportional to the square of its acceleration, which again is inverse proportional to the relative mass of the particle. The rest mass of an electron is approximately 1836 times less than a proton. Therefore, electrons are decelerated much more than protons (because of the small mass) and they are therefore the primary source of Bremsstrahlung.

Bremsstrahlung generation has been studied intensely [15]-[17]. Bremsstrahlung spectra's for electron energies from 1KeV to 10 GeV are tabulated for all matter in [17]. As an example, in figure 6 and figure 7 are shown the Bremsstrahlung spectrum for a 10 KeV and a 1 MeV electron in aluminum.

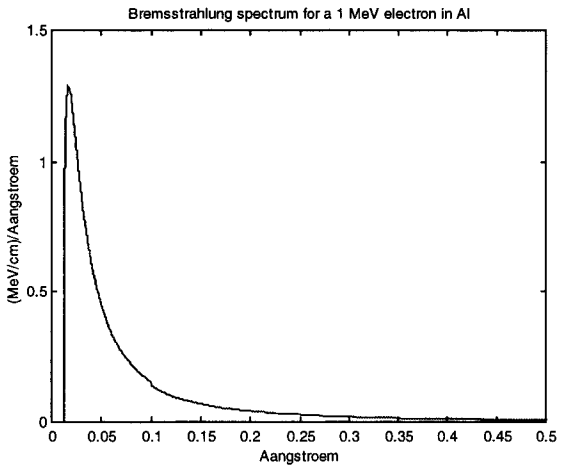

Figure 6. The Bremsstrahlung spectrum for a 1 MeV electron in Aluminum as a function of the Bremsstrahlung wavelength.

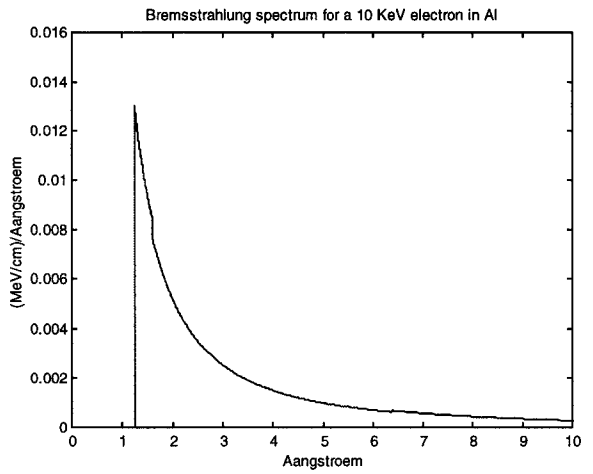

Figure 7. The Bremsstrahlung spectrum for a 10 KeV electron in Aluminum as a function of the Bremsstrahlung wavelength.

The specific Bremsstrahlung spectrum for the Europa Orbiter mission can be calculated. This is achieved, when combining the Bremsstrahlung spectra's for electron energies in the same proportions as they appear in the electron flux as shown in figure 2. The result is the relative Bremsstrahlung spectrum for the Europa Orbiter mission shown in figure 8.

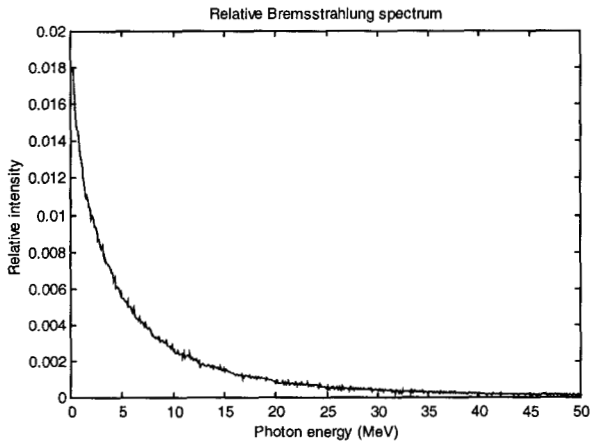

Figure 8. The relative Bremsstrahlung spectrum based on the flux from figure 2.

The Bremsstrahlung spectrum shown in figure 8 corresponds to the flux shown in figure 2, which is the flux behind $5g/cm^2$. Bremsstrahlung is generated everywhere in the shielding. This means that the outermost layer of the shielding is generating a Bremsstrahlung spectrum that is equivalent to the unshielded flux. Some of this Bremsstrahlung will penetrate though the rest of the shielding and impinge on the focal plane (it is more difficult to shield against X-rays than electrons and protons [18]). Therefore to generate a precise Bremsstrahlung spectrum, the fluxes must be known at a number of locations in the shielding (e.g. at 0.5 g/cm^2, 1.0 g/cm^2, 1.5 g/cm^2 etc.). The Bremsstrahlung spectrum generated behind $5g/cm^2$ is used in this work.

Bremsstrahlung photons will impinge on the focal plane array and some of them will interact with the focal plane array and generate charge (photoelectrons). Photons interacts with Silicon primary though 3 processes [19], [20]:

- Photoelectric effect (Low photon energy < 50 KeV)
- Compton scattering (Medium photon energy)
- Pair production (High photon energies > 10 MeV)

Only a small fraction of the Bremsstrahlung photons has energies of more than 10 MeV. Pair production is therefore not included in this work.

Photoelectric effect: In the photoelectric effect, an atom in the silicon lattice absorbs a photon and one of the silicon's orbital electrons is released. The direction of the released photoelectron is arbitrary. The energy of the photoelectron is equal to the energy of the incoming photon minus the binding energy of the orbiting electron. The binding energies for the orbital electrons in a silicon atom are [21]:

1844.1 eV	103.71 eV	13.46 eV
1844.1 eV	103.71 eV	13.46 eV
154.04 eV	103.71 eV	8.1517 eV
154.04 eV	103.71 eV	8.1517 eV
103.71 eV	103.71 eV	

The linear attenuation coefficient for the photoelectric effect is difficult to calculate theoretically. But it has been determined experimentally. Figure 9 shows a graphical representation of the linear attenuation coefficient for photons in Si [18].

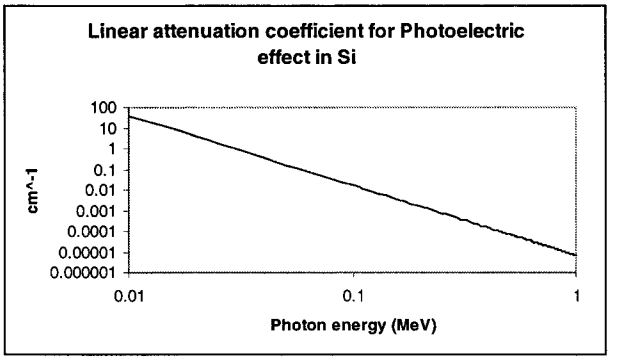

Figure 9. Linear attenuation coefficient for photoelectric effect in Silicon.

It should be emphasized that there is a fundamental difference between how charged particle and photons travel in Silicon. Charged particles interact though Coulomb forces with a huge number of other particles. Over any distance traveled, the charged particle will have interacted with millions of other particles, which continuously deflect and reduce its energy. A photon traveling in silicon does not interact with the other atoms/electrons unless a collision occurs. Therefore, it will traverse in a straight line and not loose any energy. In case of a photoelectric collision, the photon will stop to exist and all energy/momentum is transferred to the atom that it collided with.

Compton effect: The Compton effect is the phenomenon, where a photon scatters of a nearly free electron and transfers some of its energy to the electron. Equations for the linear attenuation coefficient for Compton scattering in Si are shown in [18]. Values for the linear attenuation coefficient are depicted in figure 10.

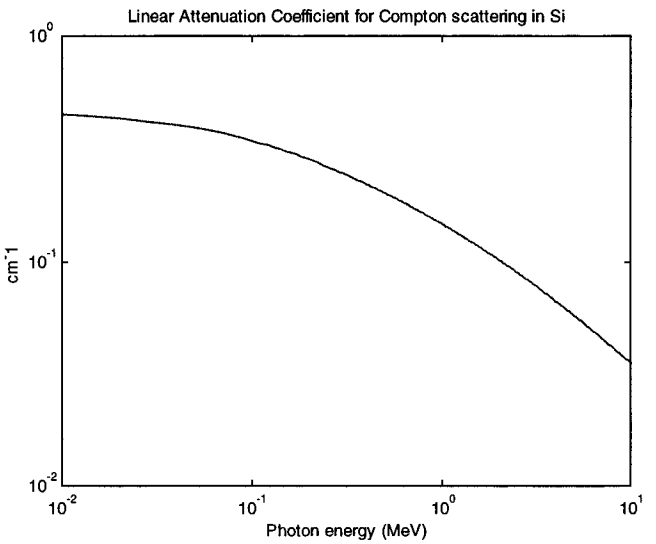

Figure 10. Linear attenuation coefficient for Compton scattering in Si.

A discussion about the distributions of the angles of the photon trajectory and the electron trajectory after the Compton collision and the energy transfer can be found in [18] and [19].

V. LUMINESCENCE

When energy is absorbed by any kind of matter, photon emissions may be the result. If the absorbed energy does not increase the thermal energy stored in the material, but changes its excited state, the emission of photons, called luminescence, results when the excited electrons give up their energy [22].

Luminescence will be emitted from the optics of a camera in a charged particle flux. Fortunately, the luminescence generated in the optics will not be focused at a specific point of the focal plane, but it will be a homogeneous glow over the focal plane.

Luminescence can be divided in two different categories, fluorescence and phosphorescence, depending on the time delay for the photon emission. If the photons are emitted less than 10 ns after the excitation the luminescence is called fluorescence; otherwise it is called phosphorescence. The emissions can be delayed for hours because the transition of excited electrons to their ground stage goes though intermediate states.

It is difficult to make an analytical model for the fraction of the deposited energy that is transformed into heat, displacement damage, luminescence etc. It depends on the material, fabrication processes etc. Viehmann et al. [23] have published the results shown in table 1, showing emitted photons per 100 nm bandwidth and per MeV of deposited energy, valid in the spectral band of 320-570 nm. The photons are emitted randomly in all directions.

Table 1

Glass type	Luminescence Photons/(100nm·MeV) in 4π sr.
Al_2O_3, Sample 1	533
Al_2O_3, Sample 2	386
Al_2O_3, Sample 3	115
Al_2O_3, Sample 4	890

Al_2O_3, Sample 5	125
Spectrosil	40
7940 glass	35
Suprasil	40
8337 glass	67
9741 glass	75
7056 glass	35

To make a reliable assessment of the Luminence, experiments must be performed with samples of the glass to be used in the optics of the camera system.

VI. CERENKOV RADIATION

Cerenkov radiation is the optical equivalent to a supersonic boom [24], [25]. It occurs when charged particles travels faster than light in a medium (e.g. glass or water). No particle can travel faster than the speed of light in vacuum. In glass with a refractive index n, a particle may travel faster than light, if $v > c/n$. If we assume that the refractive index $n = 1.4$, then this is true for electrons with energies larger than 220 KeV and protons with energies larger than 400 MeV.

Cerenkov radiation is only emitted during deceleration, and is emitted along the surface of a forward-directed cone aligned with the particle velocity vector. The wavelength of the light is mainly in the UV/blue end of the spectrum. It can be shown that the half angle of the cone is $\cos\phi = \beta'/\beta$. Where β is the velocity of the particle and β' is the velocity of light in the glass. The radiation comes from transient polarization of the medium near the charge track, and not from the particle itself.

The equation for emitted Cerenkov radiation is shown in [25]. As an example, in figure 11 and figure 12, are shown the Cerenkov radiation emission from a 300 KeV and a 10 MeV electron in a medium with a refractive index, $n = 1.5$.

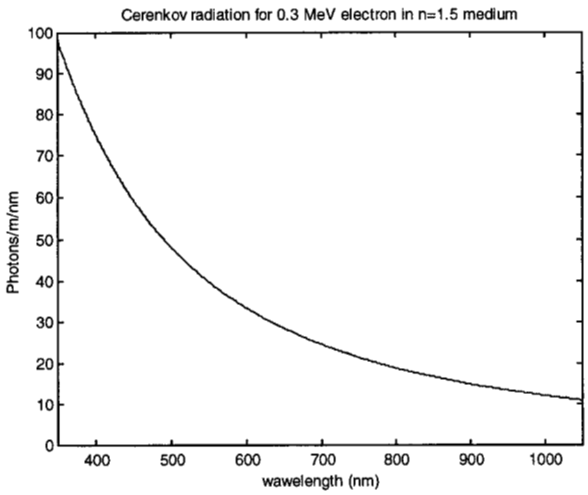

Figure 11. Cerenkov emission from a 300 KeV electron in a medium with n=1.5.

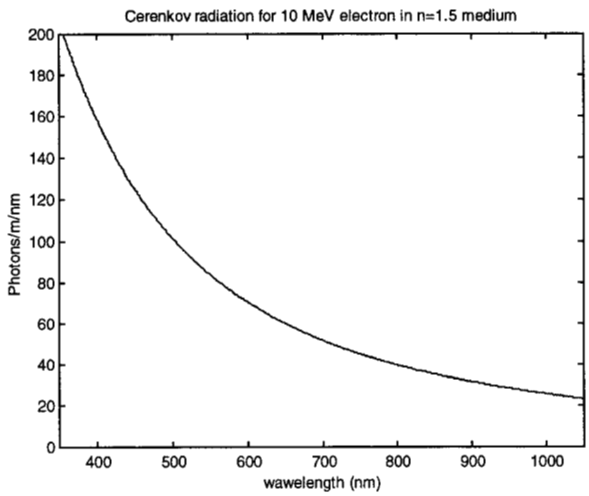

Figure 12. Cerenkov emission from a 10 MeV electron in a medium with n=1.5.

The part of the Cerenkov radiation that is actually detected by the focal plane depends on the quantum efficiency of the focal plane[2] and how the optics and focal plane is mounted relative to each other. The Cerenkov photons will not be focused on the focal plane, but will be impinging homogeneous over the focal plane.

---

[2] An example of the absolute quantum efficiency for a modern silicon focal plane array is shown in [26].

VII. FOCAL PLANE ARRAY MODEL

A simplified model of a focal plane has been constructed. The model has similarities to a front side illuminated surface channel P type CCD focal plane array. A typical CCD is manufactured from a silicon wafer, that is 500 microns thick [27], [28]. On top of the wafer an epitaxial layer is deposited with a thickness of typically 5 to 50 microns. On top of this is deposited a thin insulating layer (SiO_2) that is typically a few tenths of microns thick. Finally on top of the insulating layer, are thin electrodes, typically made of aluminum or polycrystalline silicon. Each pixel is a MOS capacitor. The gate of the MOS capacitor is positively biased. This result in all holes are pushed away from the electrode and all electrons are attracted to the electrode. The volume, under the electrode, where there are no carriers is called the depletion zone and is typically 3 – 6 microns deep depending on the bias voltage. The part of the epitaxial layer, that is not depleted, is refereed to as the diffusion (or field free) zone. The simplified model has no electrodes, since the charge generated in them does not contribute to the collected signal. The insulating layer is so thin, that it has been neglected. It is also assumed that the pixels are adjacent to each other [10]. Figure 13 shows a sketch of the simplified model.

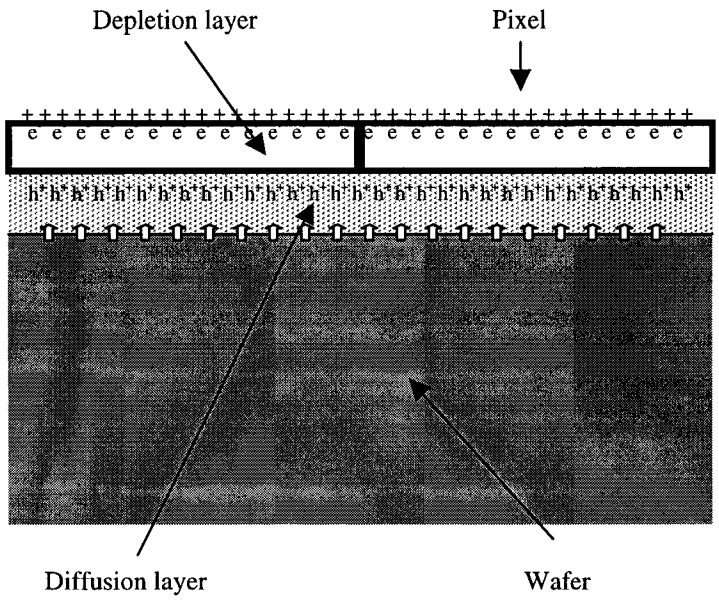

Figure 13. Sketch of the focal plane model used in the simulations. e^- are electrons and h^+ are holes.

The following assumptions have been made about the dimensions and characteristics of the focal plane array, based on average values for CCD focal plane arrays and other references [29]-[37].

- Thickness of depletion region: 4 microns
- Thickness of diffusion region: 11 microns
- Thickness of substrate >100 microns
- Diffusion length in field free region: 50 microns
- Diffusion length in substrate: 10 microns
- Pixel size: 20 microns x 20 microns

It is assumed that all minority carriers that reach the depletion zone before they recombine will be collected. It is also assumed, that all minority carries, that diffuse in the diffusion zone, and approach the substrate will be swept back into the diffusion zone due to the field between the substrate and the diffusion zone. Also, carriers generated in the substrate can freely diffuse into the diffusion zone [10].

VIII. SIMULATIONS

Three types of simulations have been performed in this work. The simulations are electrons, protons and Bremsstrahlung photons impinging on the focal plane array.

Simulation of electrons impinging on the focal plane array: This simulation was performed by selecting random electrons according to the energy distribution shown in figure 2. The electrons impinge on the focal plane model from a random direction. The electrons perform a random walk as previously described, leaving an iontrack. The deposited charge diffuse around the iontrack. The diffusion length depends on its location in the focal plane array. Finally, an image is formed, based on the number of photoelectrons collected in the depletion region. Figure 14 illustrates some representative images of electron hits.

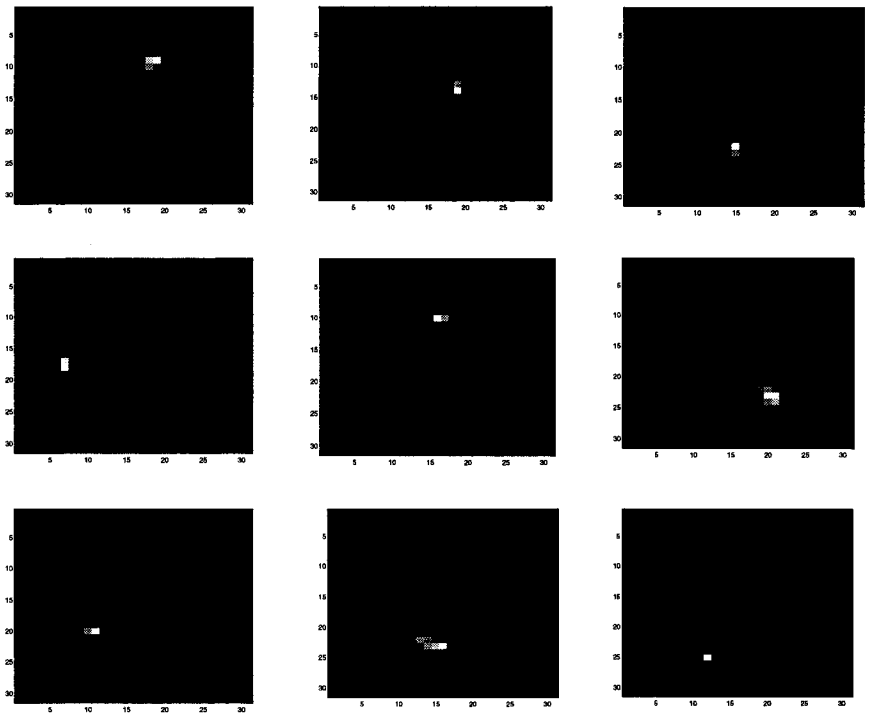

Figure 14. Sample images of electron hits. The units are in pixels.

The electron simulation shows that on average 3600 photoelectrons are collected for each impinging electron. The cumulative probability distribution is shown in figure 15. It is observed that on some occasions (99% percentile), an impinging electron may deposit more than 17000 photoelectrons as a collected signal.

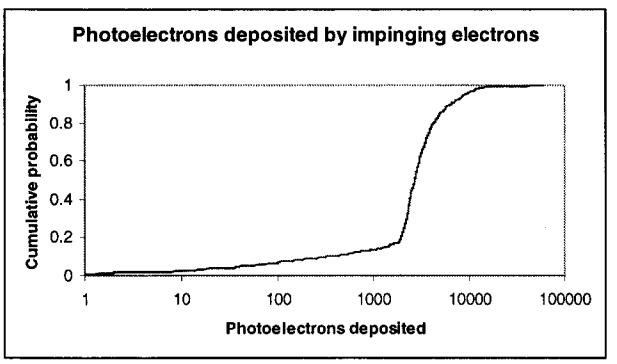

Figure 15. The cumulative probability function of number of collected photoelectrons for an impinging electron.

Simulation of protons impinging on the focal plane array: This simulation was performed, by selecting protons with a random energy according to the energy distribution shown in figure 1. The rest of the

procedure was similar to that of impinging electrons. Figure 16 shows a number of representative images generated by impinging protons.

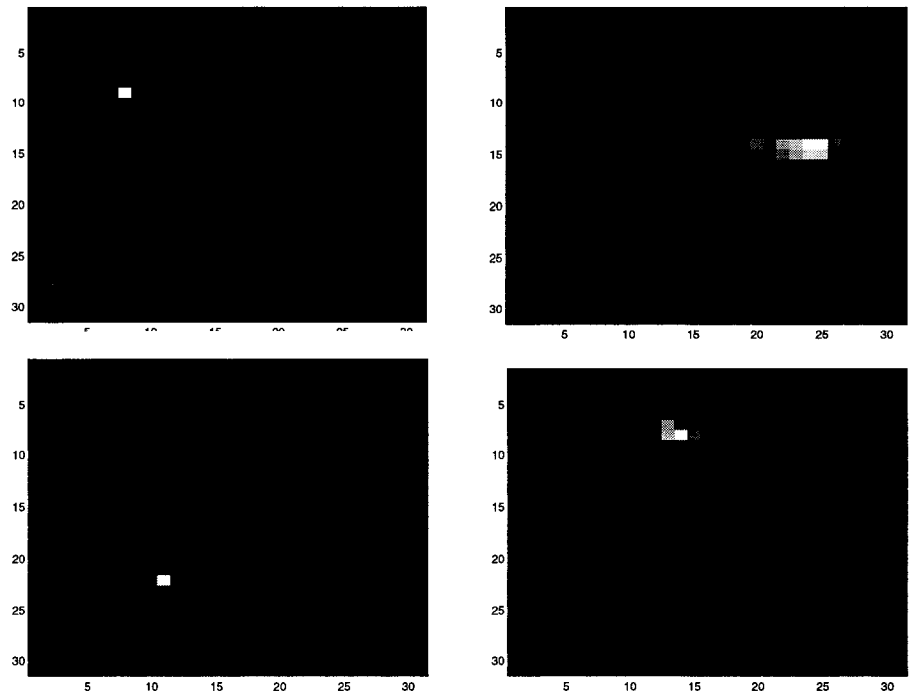

Figure 16. Sample images of proton hits. The units are in pixels.

The results of the simulation are that on average will 15000 photoelectrons be collected for each impinging proton. The cumulative probability distribution is shown in figure 17. It is observed, that on some occasions (99% percentile), an impinging proton may deposit more than 125000 photoelectrons collected as a signal.

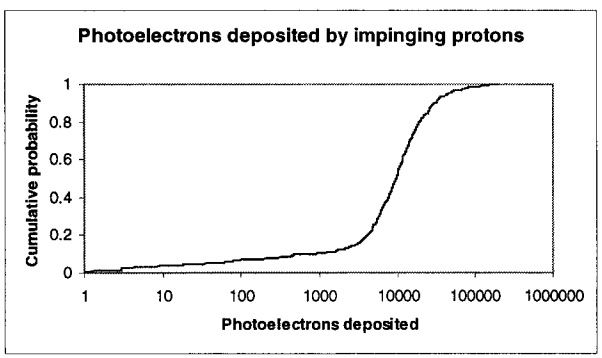

Figure 17. The cumulative probability function of number of collected photoelectrons for an impinging proton.

Simulation of Bremsstrahlung photons impinging on the focal plane array: This simulation was performed by selecting Bremsstrahlung photons with a random energy according to the spectrum shown in figure 8.

The photons impinge on the focal plane model from a random direction. They might interact with the silicon lattice, based on the linear attenuation coefficient for photoelectric effect shown in figure 9 and Compton scattering shown in figure 10 and generate electrons in the silicon. Each electron generated in the silicon is simulated similar to the method described under electrons. Figure 18 shows a number of representative images generated by Bremsstrahlung photons.

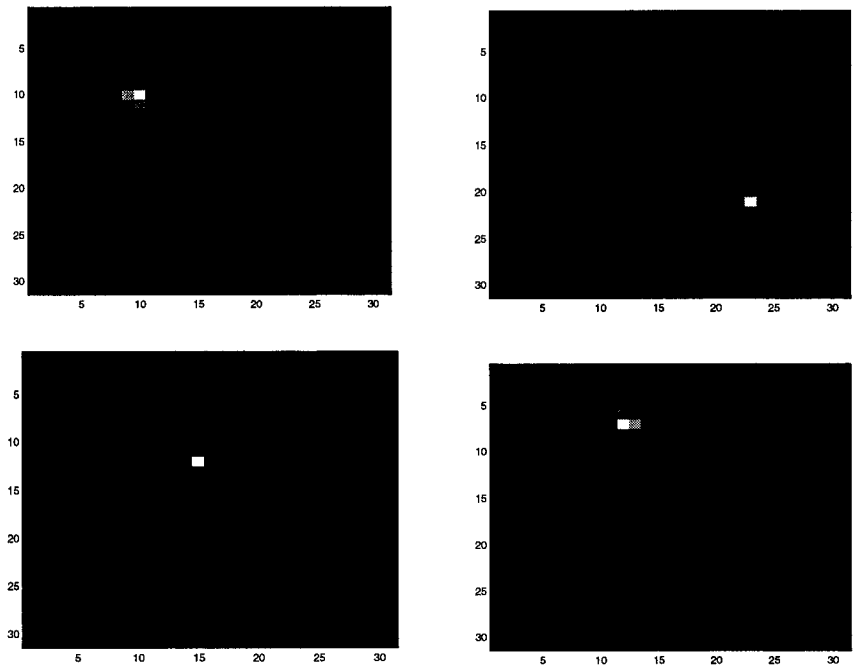

Figure 18. Sample images of Bremsstrahlung photon hits. The units are in pixels.

The Bremsstrahlung simulation shows that on average 6000 photoelectrons would be collected as a signal. The cumulative probability distribution is shown in figure 19. It is observed that on some occasions (99% percentile), an impinging Bremsstrahlung photon may deposit more than 51000 photoelectrons collected as a signal.

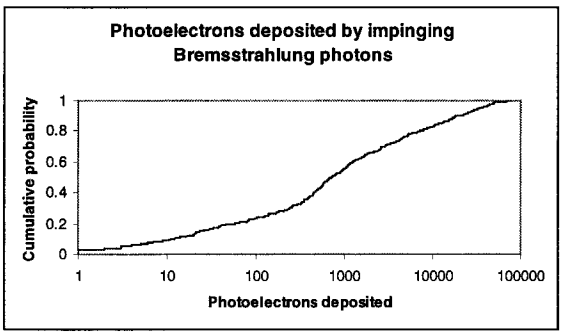

Figure 19. The cumulative probability function of number of collected photoelectrons for an impinging Bremsstrahlung photon.

It is observed, that many of the radiation hits looks similar to a small star. The absolute sensitivity of a camera system, that is imaging stars can be measured as photoelectrons collected from a magnitude 0 star with 1 second exposure time and 1 mm^2 collecting aperture. It is then possible to scale to various camera system configurations. The number 13600 $e^-/(s \cdot mm^2)$ is published in [38] for an APS based focal plane, and the number 11500 $e^-/(s \cdot mm^2)$ can be derived from [39] for a CCD based focal plane. It is assumed that the camera system has an aperture on 3 cm and integrates for 250mS. The correspondence between star magnitude and number of photoelectrons are shown in table 2. Table 2 also shows the number of stars brighter than the star magnitude.

Table 2

Magnitude (M_V)	Photoelectrons	Number of star on sky
0	$2.2 \cdot 10^6$	5
1	$8.8 \cdot 10^5$	16
2	$3.5 \cdot 10^5$	54
3	$1.4 \cdot 10^5$	183
4	$5.6 \cdot 10^4$	582
5	$2.2 \cdot 10^4$	1511
6	$9.0 \cdot 10^3$	4084

The full well of a pixel is typically in the order of 100000 photoelectrons.

IX. SUMMARY

This paper has investigated the physics of the interaction between charged particles and a focal plane array, shielding and the optics of a camera system. A simple model of a focal plane array has been constructed using typical values for pixel dimensions, diffusion lengths, depletion/diffusion layer thickness etc. Simulation using these values shows that impinging electrons with a flux similar to the Europa Orbiter environment behind 5 g/cm^2 shielding will on the average generate 3600 photoelectrons. Impinging protons from the same environment will on the average generate 15000 photoelectrons and Bremsstrahlung photons will on the average generate 6000 photoelectrons. Sample images of radiation induced spots are shown in this paper. Cerenkov radiation and Luminescence will also generate a signal in the camera optics. The signal will be spread homogeneous over the focal plane. Bright radiation hits have similar shape and brightness as dim stars.

X. ACKNOWLEDGEMENTS

The author would like to thank Randall K. Bartman and Curtis Padgett, JPL for reviewing this paper.

The research described here was carried out at the Jet Propulsion Laboratory, California Institute of Technology, and was sponsored by the National Aeronautics and Space Administration. References herein to any specific commercial product, process or service by trademark, manufacturer, or otherwise, does not constitute or imply its endorsement by the United States Government or the Jet Propulsion Laboratory, California Institute of technology.

XI. REFERENCES

[1] Konrad Kleinknecht: Detectors for Particle Radiation, Cambridge University press, England, 1998, ISBN: 0521640326.

[2] EG&G ORTEC: Detectors & Instruments for Nuclear Spectroscopy 91/92, ii-4, EG&G ORTEC, United States, TN 37831, 1991.

[3] G.R.Hopkinson, C.J.Dale and P.W.Marshall: Proton Effects in Charge-Coupled Devices, IEEE transactions on nuclear science, Vol. 43, No. 2, April 1996.

[4] Geoffrey P.Summers, Edward A. Burke and Robert J. Walters: Damage Correlations in semiconductors exposed to gamma, electron and proton radiation, Nuclear Science, IEEE Transactions on Volume: 40 6 1-2, Dec. 1993, Page(s): 1372 –1379.

[5] C.C.Liebe et al: Star Tracker Design Considerations for the Europa Orbiter Mission, 1999 IEEE Aerospace Conference, Aspen, CO, Mar. 6-13, 1999, Proceedings. Vol. 2, p. 67-81.

[6] Nicholas Tsoulfanidis: Measurement and Detection of Radiation, Hardcover 2nd edition (March 1995), Taylor & Francis; ISBN: 1560323175.

[7] John David Jackson: Classical Electrodynamics, 2nd Edition, (October 3, 1975) John Wiley & Sons, ISBN: 047143132X.

[8] Scott Kirkpatrick: Modeling Diffusion and Collection of Charge from Ionizing Radiation in Silicon Devices, IEEE Transactions on electron devices, Vol. ED-26, No. 11, Nov 1979, p.1742-1753.

[9] Larry D. Edmonds: A Graphical Method for estimating Charge Collected by Diffusion from an Ion track: IEEE transactions on Nuclear Science, Vol. 43, No. 4, August 1996, p. 2346-2357.

[10] Gordon R. Hopkinson: Analytic modeling of charge diffusion in charge-coupled device imagers, Optical Engineering 26(8), p. 766-772 (August 1987).

[11] David H. Seib: Carrier Diffusion Degradation of Modulation Transfer Function in Charge Coupled Imagers, IEEE Transactions on electron devices, Vol. ED-21, No. 3, March 1974, p.210-217.

[12] J.A. Zoutenduk, H.R.Schwartz and L.R.Neville: Lateral Charge Transport From Heavy-Ion tracks in integrated Circuit chips, IEEE Transactions on Nuclear Science, Vol. 35, No. 6, December 1988, p. 1644-1647.

[13] Robert F. Pierret: Semiconductor Device Fundamentals, (March 1996) Addison-Wesley Pub Co, ISBN: 0201543931.

[14] Joseph M. Pimbley and Gerald J. Michon: Charge Detection Modeling in solid-state Image Sensors. IEEE Transactions on electron devices, Vol. ED-34, No. 2, February 1987, p.294-300.

[15] Stephen M. Seltzer and Martin J. Berger: Bremsstrahlung spectra from electron interactions with screened atomic nuclei and orbital electrons, Nuclear Instruments and Methods in Physics Research B12 (1985) p. 95-134.

[16] Lucien Pages et al: Energy Loss, Range, and Bremsstrahlung Yield for 10 KeV to 100 MeV electrons in various elements and chemical compounds, Atomic Data 4, p. 1-127, 1972.

[17] Stephen M. Seltzer and Martin J. Berger: Bremsstrahlung energy spectra from electrons with kinetic energy 1 KeV-10 GeV incident on screened nuclei and orbital electrons of neutral atoms with Z= 1-100, Atomic Data and Nuclear Data Tables 35, p. 345-418, 1986.

[18] Kenneth S. Krane: Introductory Nuclear Physics, John Wiley & Sons, ISBN: 047180553X, 1987.

[19] Robley D. Evans: Gamma Rays, American Institute of Physics Handbook, p. 8.190-8.205, McGraw-Hill Book Company, New York.

[20] Ellery Storm and Harvey I. Israel: Photon Cross Sections from 1KeV to 100 MeV for elements Z = 1 to Z = 100, Nuclear Data Tables, A7, p. 565-681 (1970).

[21] http://www.colorado.edu/physics/2000/periodic_table/index.html

[22] Robert M. Besancon: The Encyclopedia of physics, Von Nostrand Reinhold Company, New York, 1985, p. 669-674.

[23] W. Viehmann et al: Photo multiplier window materials under electron irradiation: fluorescence and phosphorescence, Applied Optics, Vol. 14, No. 9, p. 2104-2115. Sep. 1975.

[24] J.V.Jelley, Cerenkov radiation, and its applications. Published for the United Kingdom Atomic Energy Authority. New York, Pergamon Press, 1958.

[25] Arthur H. Snell: Nuclear Instruments and their uses, John Wiley and Sons Inc., New York, 1962.

[26] http://www.kodak.com/US/en/digital/ccd/kaf0401LE.shtml

[27] Christian Buil: CCD Astronomy, Construction and Use of an Astronomical CCD Camera, Willmann-Bell, ISBN: 0943396298, 1991.

[28] Morley M. Blouke: Charge-Coupled Devices, Encyclopedia of Applied Physics, Vol. 3., VCH Publishers Inc, 1992, p.241-272.

[29] Thomson-CSF: Hardening of CCD Image Sensors, Thomson-CSF Semiconducteurs Specifiques, B.P. 123, 38521 Saint-Egreve Cedex, France.

[30] J.P.Spratt, B.C.Passenheim, R.E.Leadon: The effects of Nuclear Radiation on P-Channel CCD imagers, IEEE Radiation effects data workshop, NSREC, Snowmass 1997, Workshop record.

[31] Caranhac, S.; Coutures, J.L: Comparative evolution of various CCD image sensors hardening techniques with ionizing radiation, Radiation and its Effects on Components and Systems, 1993, RADECS 93, Second European Conference on, 1994, Page(s): 396–400.

[32] T. Roy, S.J.watts and D. Wright: Radiation damage effects on imaging charge-coupled devices, Nuclear Instruments and Methods in Physics Research A275 (1989), p. 545-557.

[33] George J. Yates and Bojan T. Turko: Circumvention of radiation induced noise in CCD and CID imagers, IEEE Transactions on nuclear science, Vol. 36, no. 6, December 1989, p. 2214-2222.

[34] Allan Owens and Kieran J. McCarthy: Energy deposition in X-ray CCDs and charged particle discrimination, Nuclear Instruments and Methods in Physics Research A366 (1995), p. 148-154.

[35] Andrew Chugg and Gordon Hopkinson: A new Approach to modeling Radiation Noise in CCDs, IEEE Transactions on nuclear Science, vol. 45, No. 3, June 1998.

[36] T.S.Lomheim et al: Imaging charge coupled device (CCD) transient response to 17 and 50 MeV proton and heavy-ion irradiation, IEEE Transactions on Nuclear science, Vol. 37, No. 6, Dec 1990, p. 1876-1885.

[37] M.S.Robbins, T.Roy and S.J.Watts: Degradation of the Charge Transfer Efficiency of a Buried Channel Charge Coupled Device Due to Radiation Damage by a Beta Source, IEEE proceedings of First European Conference on Radiation and its Effects on Devices and Systems (RADECS'91), La Grande-Motte, September 1991, Vol. 45, p. 327-332.

[38] C.C.Liebe, E.W.Dennison, B.Hancock, R.C.Stirbl, and B.Pain: Active Pixel Sensor (APS) based Star Tracker, Proceedings of IEEE Aerospace conference, Aspen 1998, fp242.pdf.

[39] R.H.Stanton et al: ASTROS: A sub-arcsec CCD Star Tracker, SPIE/Vol. 501, State of the Art Imaging Arrays and Their Application (1984).